PIER B

Bandwidth Enhancement Methods Analysis for High-Gain Stacked Microstrip Antenna

Mikhail S. Shishkin*

*Ural Federal University named after the first President of Russia B. N. Yeltsin
(Engineering School of Information Technologies, Telecommunications and Control Systems)
Yekaterinburg, Russia*

ABSTRACT: This article presents the results of bandwidth enhancement method analysis for a stacked microstrip antenna. Based on the analysis results, a new design of a wideband, compact, high-strength antenna is proposed. The antenna operates in a wide frequency band of 4660 to 6048 MHz ($\sim 26\%$) with an impedance bandwidth matching of 15 dB; throughout its whole operating frequency range, the antenna gain is from 11 to 13.4 dBi. The antenna allows it to form a specific shape of radiation pattern with coverage predominantly in the upper (lower) hemisphere and a fixed main lobe deflection angle about 4 degrees in the elevation plane. The antenna consists of a wideband E-shaped active exciter and four passive rectangular exciters placed above the conductive plane (screen). All elements are made of sheet metal (e.g., stainless steel). The antenna size is $1.4\lambda_{max} \times 1.4\lambda_{max}$ ($1.6\lambda_0 \times 1.6\lambda_0$). The analysis of the characteristics of the designed antenna was performed using simulation in the ANSYS EM Suite. A prototype was made, and its properties were measured. The proposed antenna may be designed with a different frequency band with a matching band about 25% and can be used as a wireless communication system repeater or small cell antenna, as a ground station antenna in unmanned aircraft systems, or for other wideband applications with high gain.

1. INTRODUCTION

In the field of mobile communications, the use of wideband and multi-band antennas has advanced significantly over the past two decades. These antennas, designed for the use in mobile devices, repeaters, and base stations, exhibit a wide range of shapes and sizes adapted for specific radiation pattern (RP) requirements. Throughout this period, numerous research studies have been conducted, and a great number of noteworthy studies, articles, and books have been spread within this field. Various methods have been proposed to expand the operating frequency band of antennas, for example [1–46]. Nonetheless, as robotic systems grow at a rapid pace, there is a renewed interest in antenna research.

The development of diverse robotic systems, most notably unmanned aerial systems (UASs), represents an exceptional and rapidly advancing technological frontier. A conventional UAS is made up of a ground control station (GCS) and several unmanned aerial vehicles (UAVs). The standard wireless propagation channel of a UAS can be separated into two categories:

- payload communications, which can be narrowband or wideband (application-dependent);

- control and non-payload communications (CNPC) for telemetric control of UAVs.

The payload communication channel is often referred to as the Intelligence Surveillance and Reconnaissance Data Link. A Command-and-Control Data Link (C2DL) is essentially the same as CNPC. Typically, the function of C2DL is to provide a command-and-control uplink and a telemetry downlink for single or multiple UAVs, a limited narrow band sensor downlink for UAV sensors, voice communication, and a network-enabled capability to support multi-node communication. UAS conducts wireless communication in both civilian and military contexts by using sufficiently wide frequency bands. When wireless communication is organized between a GCS and a UAV, a major challenge is to provide radio communication at a certain distance, while the GCS antenna must ensure radio coverage in a certain fixed area [5, 47].

The article presents the design of an antenna operating in the wide frequency band of 4660 to 6048 MHz ($\sim 26\%$). The antenna gain is 11–13.4 dBi. Meanwhile, unlike an antenna array, it is small in size ($1.4\lambda_{max} \times 1.4\lambda_{max}$ or $1.6\lambda_0 \times 1.6\lambda_0$) and does not require a complex feeding network. The proposed antenna can be used as a wireless communication system repeater or small cell antenna as a ground station antenna in unmanned aircraft systems or other wideband applications with high gain. The analysis of techniques for expanding the antenna frequency band, initially mentioned in [44], provides the basis of the newly proposed wideband high-gain antenna design.

2. THE MICROSTRIP ANTENNAS OPERATING FREQUENCY BAND EXPANDING METHODS

An antenna is considered wideband if its matching band (bandwidth) is as follows for a specific level of voltage standing wave

* Corresponding author: Mikhail S. Shishkin (mikkhail666@gmail.com).

ratio or reflection coefficient (S_{ii} magnitude) [5]:

$$\text{BW} = \frac{f_u - f_l}{f_c} \cdot 100\% = 2 \cdot \frac{f_u - f_l}{f_u + f_l} \cdot 100\% \geq 10\%, \quad (1)$$

where f_u is the upper frequency of the operating range, f_l the lower frequency of the operating range, and f_c the central frequency of the operating range.

Some options to increase the operating frequency band of patch antennas were considered in [1–46]. A means to enhance the matching bandwidth of a patch antenna is to use a passive element rather than an active one, resulting in an electromagnetically coupled patch antenna (ECPA). There are several research papers that explore this technique, including [1–5]. Through the implementation of this approach, the antenna matching band can be expanded to approximately 15–20%. These antennas typically exhibit gains ranging from 5 to 7 dBi. It is possible to increase the matching bandwidth of antennas by more than 20% by using different feed methods, as shown, for example, in [5], where a bandwidth about 33% was achieved with uniform characteristics in the operating frequency band.

Through the precision cutting of slits in a defined shape in the radiating patch, one can effectively broaden the working band of a microstrip antenna [6–13]. The most popular of these antennas are the so-called U-shaped and E-shaped microstrip antennas, extensively documented in [14] and [15]. By using an air substrate in such antennas, it is possible to achieve a matching bandwidth up to 30% and more with a maximum gain of 7–7.5 dBi.

In addition to the methods discussed above, there are various forms of microstrip antennas that make it possible to obtain a wide or ultra-wide matching band, for example [16–25]. As we can see from [1–25], the gain of a single antenna is, as a rule, quite low and does not exceed 7–8 dBi; it can be increased by combining wideband elements into an antenna array, which requires the use of a broadband feed network. However, it should be remembered that a wideband feed network can be quite complex in terms of design and implementation [1, 22–31]. Therefore, it is necessary to consider the possibilities of increasing the gain of wideband antennas without combining them into an antenna array.

The designs of antennas where the authors were able to achieve high gain in the wide frequency range without a complex feed network can be found in [32–46]. For example, in [32–35] it was possible to increase the gain of wideband antennas due to the design of the exciter itself and its optimal location above the conducting screen. The disadvantages of these methods are the complexity of the design and low level of matching, and the gain is not higher than 10–11 dBi, although in [35] it was possible to achieve a peak gain of 12.2 dBi with an antenna matching bandwidth of 25% with $|S_{11}| \leq -15$ dB.

In [36] and [37], to increase the gain, individual exciters are located one after another in a special way, creating something like a linear array. Using this method, the authors managed to achieve gains of 12.5 and 14.5 dBi. The main drawback of the proposed technique is the large linear size of the antenna, which in the first case is $4.8\lambda_0$ and in the second one is $6.8\lambda_0$.

Adding passive (parasitic) elements to the substrate in the same plane next to the active exciter allows the antenna's operating band to be expanded [38, 39]. Alternatively, the passive elements may be connected to the active elements via transmission lines. This technique enables an antenna matching bandwidth up to 15% and a gain up to 10 dBi. To improve the characteristics of such an antenna, alternative options with different forms of both active and passive elements are proposed [40–43]. For example, using an octagon parasitic patch, the authors were able to achieve an antenna matching band of 16% [40], and in [42], due to the shape of the exciters, the authors obtained a circular polarization field.

A method for achieving a high gain (up to 12–13 dBi) while expanding the antenna matching band was presented in [44], which involved adding four passive elements at the corners of the active rectangular element at a greater height above the screen. This technique enables an antenna matching bandwidth of no more than 10–12%. In [45] and [46], modifications of this method were proposed, where the authors increased the efficiency of the antenna in frequency ranges above 60 GHz. Thus, in the design from [46], it was possible to achieve an antenna matching bandwidth of 27.3% ($|S_{11}| \leq -10$ dB) with a maximum gain of 10.5 dBi.

As can be observed, the field of study of wideband high-gain antennas is quite extensive; nevertheless, the methods discussed have their disadvantages, which indicates the need for further research on this topic.

3. ANTENNA WITH FOUR PASSIVE ELEMENTS ANALYSIS

The methods under study for obtaining high gain from a microstrip antenna in a wide frequency range are based on the design proposed in [44]. In this particular methodology, against [44], the antenna elements are made on a sheet metal basis without the use of a dielectric substrate and attached to the screen through metal racks (Figure 1) positioned at points of zero potential thereby ensuring that the characteristics of its radiation remain largely unaltered. This approach improves the directivity of microstrip antennas of round or rectangular shape and obtains a more durable structure than antennas based on a dielectric substrate [48].

The studied high-gain antenna dimensions can be calculated based on well-known expressions [49, 50]:
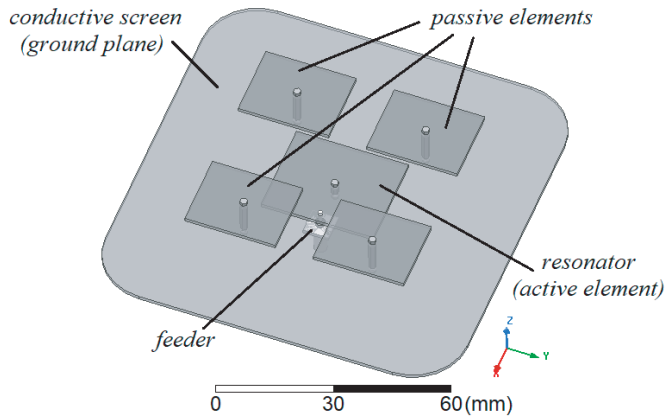
1. The non-resonant side length of the active rectangular exciter is calculated:

$$b = \frac{\lambda_0}{2\sqrt{\varepsilon}}, \quad (2)$$
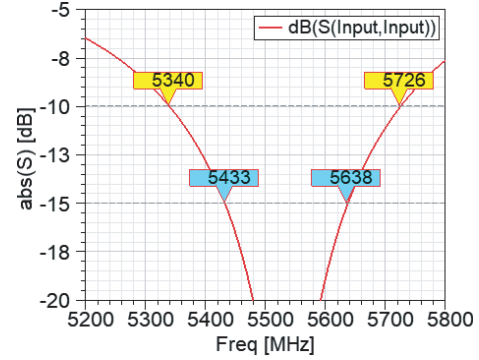
where λ_0 is the free-space wavelength at the center frequency of the operating range; ε is the substrate relative permeability.

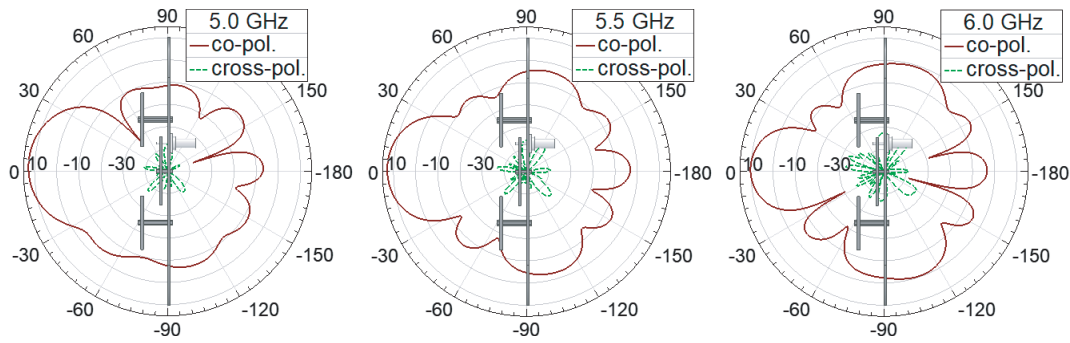2. The resonant side length of the active rectangular exciter is calculated:

$$a = b - 2\Delta, \quad (3)$$

FIGURE 1. The antenna with a rectangular active exciter and four rectangular passive elements.

FIGURE 2. The simulation reflection coefficient magnitude of the antenna with a rectangular active exciter and four rectangular passive elements.

FIGURE 3. The simulation directivity of the antenna with a rectangular active exciter and four rectangular passive elements.

where

$$\Delta = 0.412 \cdot h \cdot \left| \frac{\varepsilon_{eff} + 0.3 \cdot \frac{b}{h} + 0.262}{\varepsilon_{eff} - 0.258 \cdot \frac{b}{h} + 0.813} \right|, \qquad (4)$$

where h is the height of the active rectangular exciter above the screen (substrate thickness); ε_{eff} is the effective dielectric constant of a microstrip transmission line with the same width as the non-resonant side length of the exciter:

$$\varepsilon_{eff} = \frac{\varepsilon + 1}{2} + \frac{\varepsilon - 1}{2} \cdot \left(1 + \frac{10 \cdot h}{b} \right)^{-1/2}. \qquad (5)$$

3. The location of the feed point is determined as the distance from the center of the resonator:

$$x = \frac{a}{\pi} \sin^{-1} \sqrt{\frac{R_i}{R_e}}, \qquad (6)$$

where R_i is the required input resistance (50 Ohm), and R_e is the input resistance at the edge of the resonator:

$$R_e = \frac{1}{2G_e}, \qquad (7)$$

where G_e is the radiation conductance of resonator:

$$G_e = \frac{\pi}{377} \cdot \frac{a}{\lambda_0}. \qquad (8)$$

4. The sizes of passive elements are calculated similarly, only with a frequency 5–10% higher than the central one.

5. After the calculations, the main dimensions of the antenna are optimized to obtain the required properties in the simulation software. It is important to correctly position the passive elements, select the height of their installation above the screen, and determine the distance from the active one. Passive elements affect the active one and its input impedance, while increasing the distance allows one to restrict the radiation pattern's beam and obtain a higher gain.

As an example, consider the antenna calculated for a central frequency of 5500 MHz. The antenna simulation was carried out in the ANSYS EM Suite (HFSS Design). The compromise between the matching bandwidth and achievable gain can be found by modeling and selecting the optimal dimensions of the antenna design. The simulation results obtained for the antenna presented in Figure 1 are shown in Figures 2 and 3. As we can see, the antenna has a stable directivity of 10–13 dBi in the wide frequency band (more than 5–6 GHz, or 18%). However, the antenna has a very narrow impedance bandwidth matching,
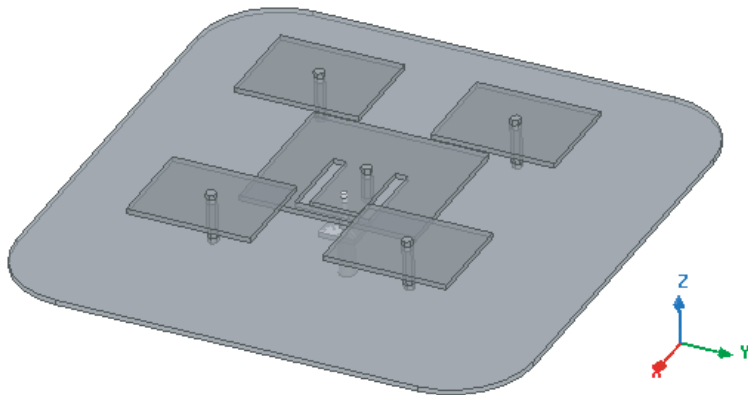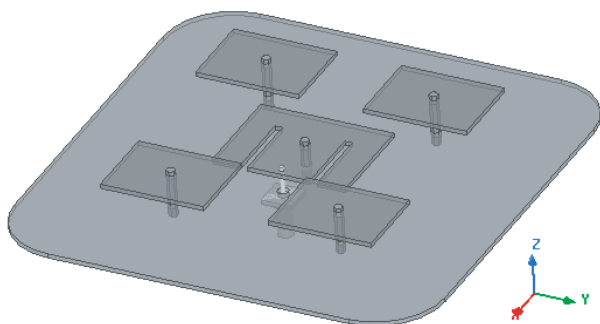
FIGURE 4. The antenna with a U-shaped active exciter and four rectangular passive elements.
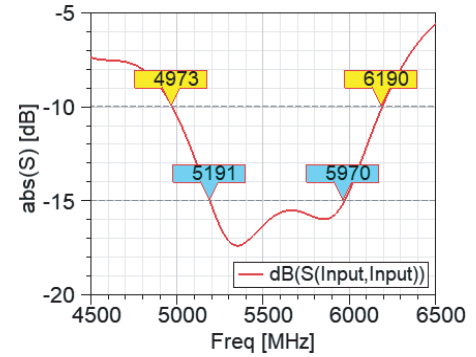
FIGURE 5. The simulation reflection coefficient magnitude of the antenna with a U-shaped active exciter and four rectangular passive elements.
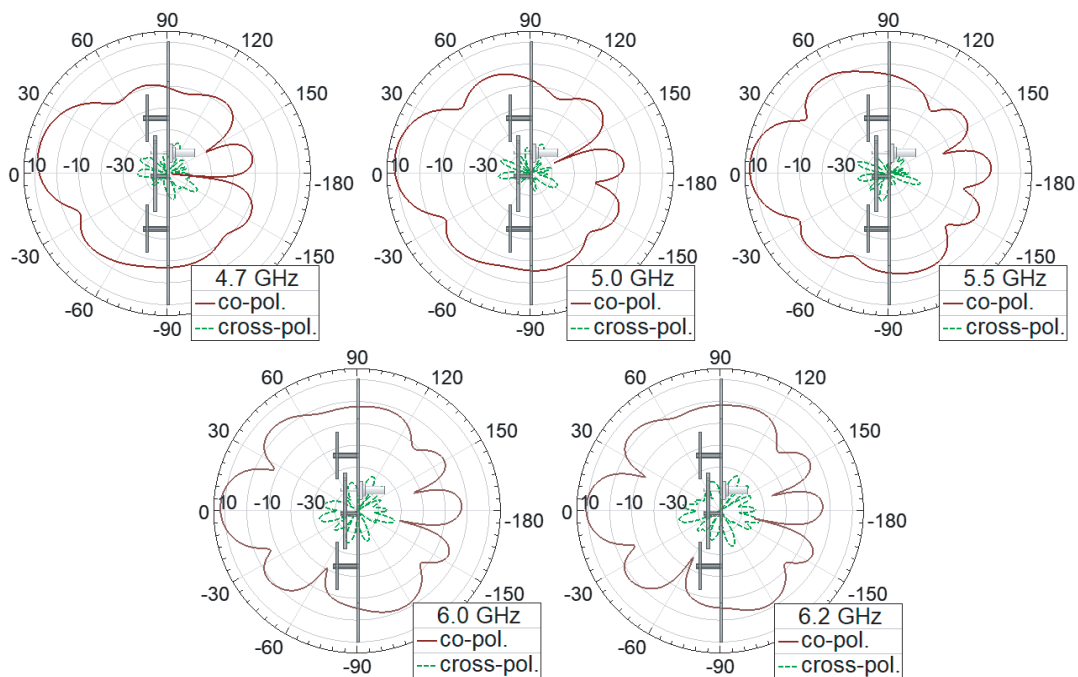
FIGURE 6. The simulation directivity of the antenna with a U-shaped active exciter and four rectangular passive elements.

FIGURE 7. The antenna with an E-shaped active exciter and four rectangular passive elements.

which is about 7% with $|S_{11}| \leq -10$ dB and less than 4% with $|S_{11}| \leq -15$ dB.

In other words, the antenna provides a higher directivity over a wider frequency band than it is possible with matching. Assumption: It is possible to ensure the operation of the antenna with a high gain in a wider frequency band than the original design from [31], on the basis of which the model in Figure 1 is created, by increasing the matching bandwidth of the active resonator without altering the design of the passive ones or the antenna's principle of operation. Next, let us consider the two simplest methods of expanding the studied antenna frequency band.

4. ANTENNA BASED ON A U-SHAPED ACTIVE EXCITER

An uncomplicated method to expand the operating frequency band of a microstrip rectangular antenna involves the inclusion
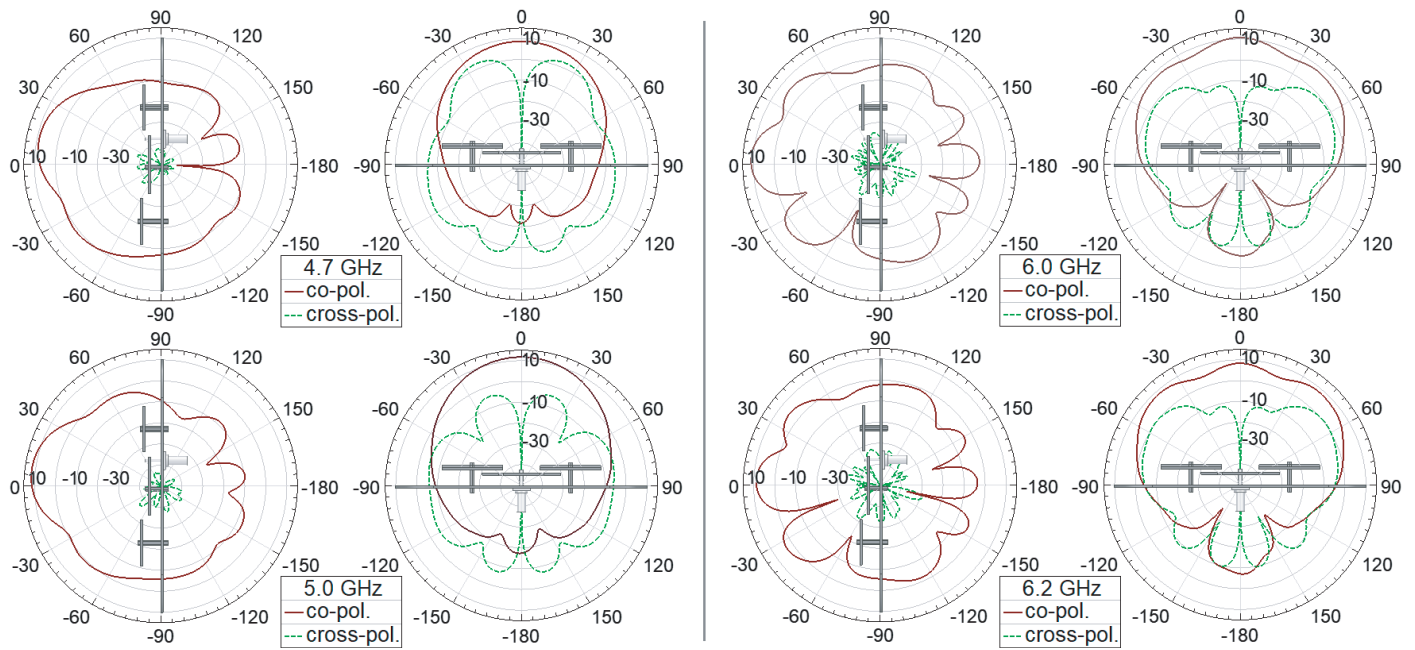
FIGURE 8. The simulated gain patterns of the antenna with an E-shaped active exciter and four rectangular passive elements.
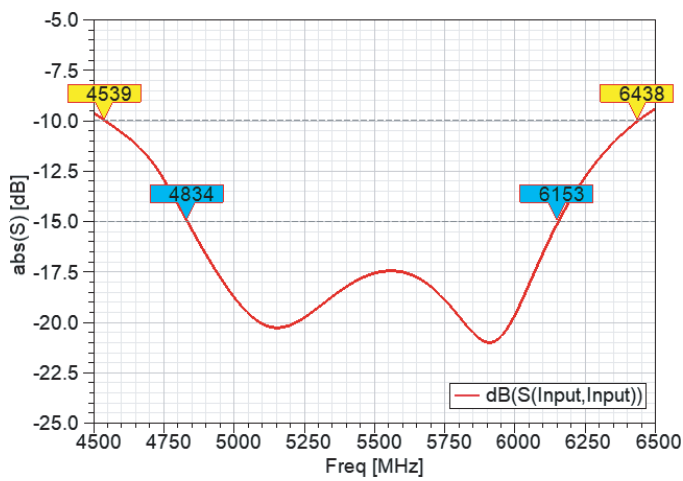

FIGURE 9. The simulated reflection coefficient magnitude of the antenna with an E-shaped active exciter and four rectangular passive elements.

FIGURE 10. The prototype of the proposed wideband antenna based on an E-shaped active exciter.

FIGURE 11. The measured reflection coefficient magnitude of the proposed wideband antenna.
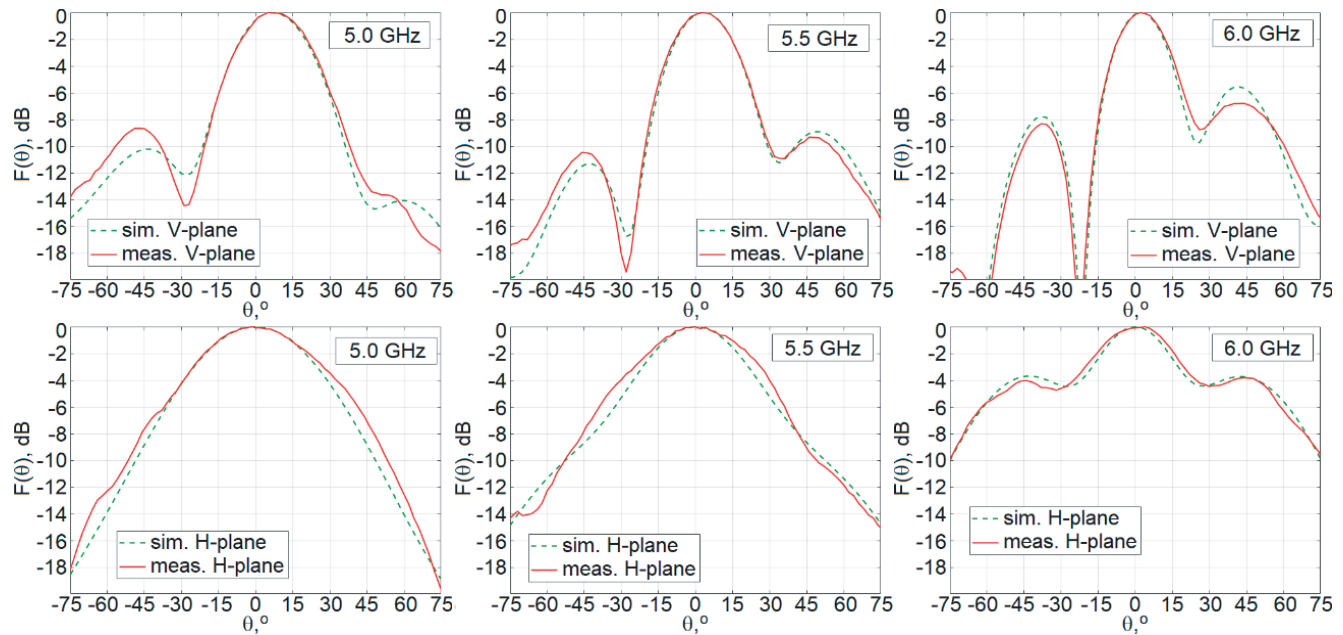
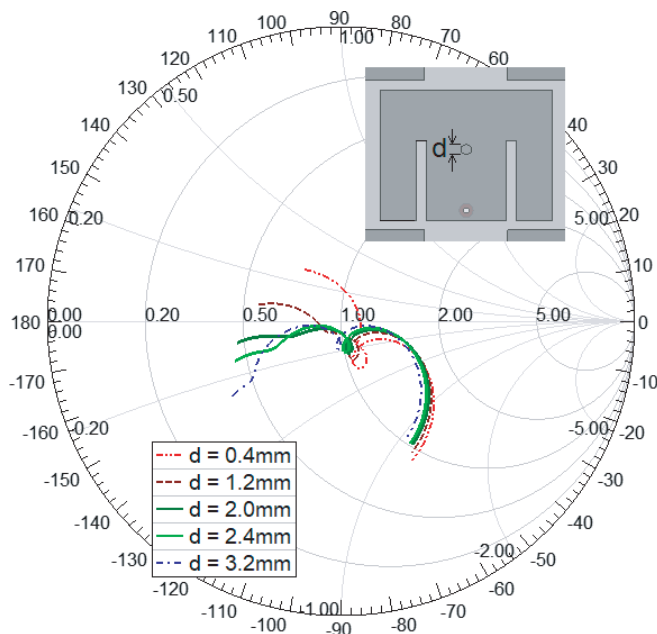FIGURE 12. The radiation patterns of the proposed wideband antenna.

FIGURE 13. The influence of the diameter of the active exciter metal rack on antenna matching.

of a U-shaped slot within the resonator's plane, known as the U-shaped patch [15] and [16]. In order to expand the operating frequency band of this antenna under investigation, it is suggested that the active exciter be substituted with a wideband U-shaped patch. The external appearance of this antenna can be observed in Figure 4, while detailed simulation results are depicted in Figures 5 and 6.

According to the results collected from the simulation, it is revealed that the suggested antenna with a U-shaped ac-

tive exciter and four rectangular passive elements possesses specific parameters of note: the antenna's directivity spans a range of approximately 9.5 to 13 dBi across a wide frequency band extending from over 4700 to 6200 MHz; in addition, its impedance bandwidth matching is estimated at 22% with $|S_{11}| \leq -10\,\text{dB}$ and 14% with $|S_{11}| \leq -15\,\text{dB}$; remarkably, the cross-polar discrimination (XPD) exceeds more than 50 dB.

5. ANTENNA BASED ON AN E-SHAPED ACTIVE EXCITER

## 5.1. Antenna Simulation Results

Another way to extend the operating frequency band of the studied high-gain antenna is to use an E-shaped patch as an active exciter (Figure 7). The simulation results of such an antenna are shown in Figures 8–9. The antenna displays exceptional performance: the operating bandwidth is around 35% (4539–6438 MHz) with $|S_{11}| \leq -10\,\text{dB}$ and 24% (4834–6153 MHz) with $|S_{11} \leq -15\,\text{dB}$; the gain is 10 to 13 dBi in the wide frequency band 4767–6069 MHz (24%) with an impedance bandwidth matching of 10 to 15 dB; the RP of the antenna has a specific shape, with coverage predominantly in the upper hemisphere, a fixed main lobe about 4° in the elevation plane, and a symmetrical shape in the azimuth plane. The XPD exceeds 50 dB when being directed towards its maximum radiation.

5.2. Antenna Measurements Results

An image of the manufactured wideband antenna prototype is shown in Figure 10.
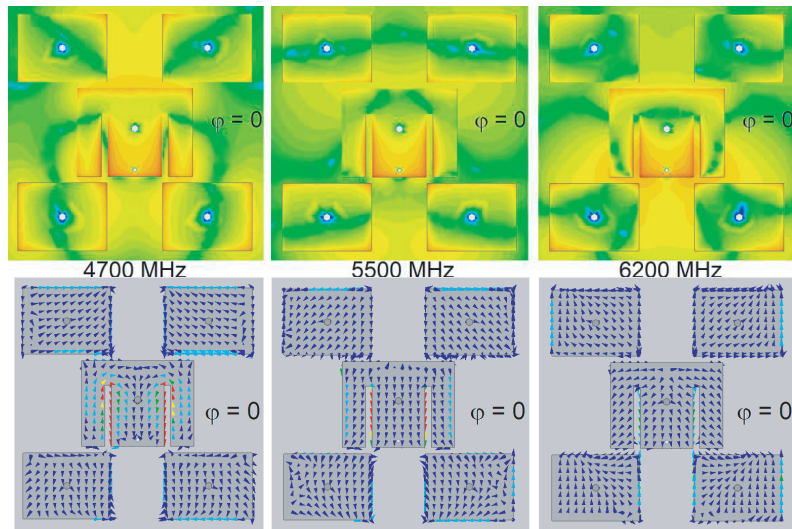
FIGURE 14. The E-field distribution and the current distribution over the antenna elements surfaces.
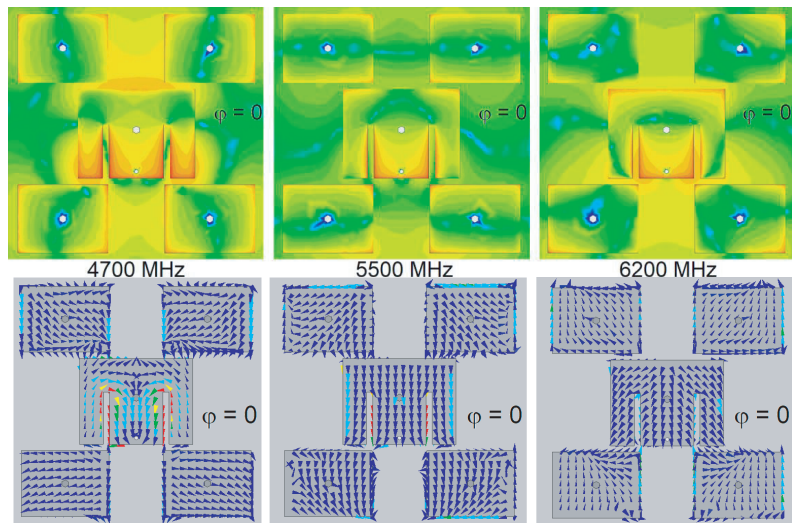
FIGURE 15. The E-field distribution and the current distribution over the optimized antenna elements surfaces.

A 1 mm stainless steel sheet was used as the material for the antenna elements. All antenna elements (screen, active, and passive exciters) are manufactured using laser cutting with an accuracy of not less than 0.1 mm. The exciters are connected to the ground plane via brass racks for printed circuit boards with diameter of 2.5 mm, which, depending on the model, provide the distance to the screen. The SMA-Female connector is soldered to the active E-shaped patch with a central conductor, and the connector is soldered to the screen with the outer conductor. The measurement results are shown in Figures 11 and 12.

According to the obtained data, the shapes of the radiation patterns are similar to those obtained in the simulation. The measured reflection coefficient curve is close to those obtained in the simulation, but shifted upward in frequency. These differences may be caused by inaccuracy in the manufacture of the antenna elements. The measured impedance matching band-width is 25% (from 5082 to 6556 MHz) with $|S_{11}| \leq -15$ dB and about 39% (from 4683 to 6938 MHz) with $|S_{11}| \leq -10$ dB.

5.3. Proposed High-Gain Antenna Optimization

Unlike the design shown in Figure 1, the metal rack for mounting the active E-shaped exciter is not located at the point of zero potential, and its diameter and location affect the antenna characteristics. Figure 13 shows the effect of rack diameter on the antenna input impedance. As can be seen from the Figure, increasing the diameter of the rack shifts the frequency range of the antenna to the right and narrows it.

Figure 14 depicts the distribution of Efields and currents over the surfaces of the antenna exciters, derived from simulation results. The uniform distribution of the field over the surface of all antenna elements is impacted by the metal racks in the
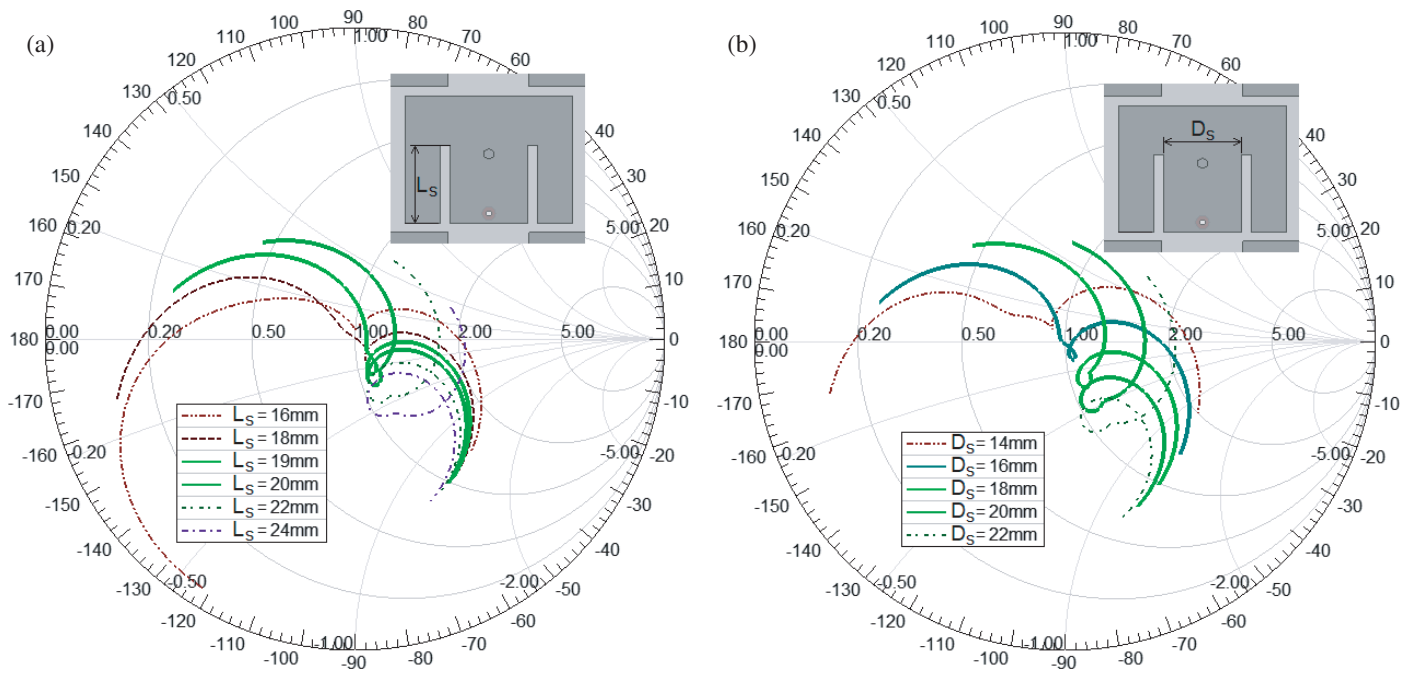
FIGURE 16. (a) The slots length and (b) the distance between the slots influence on the input characteristics of the studied antenna.
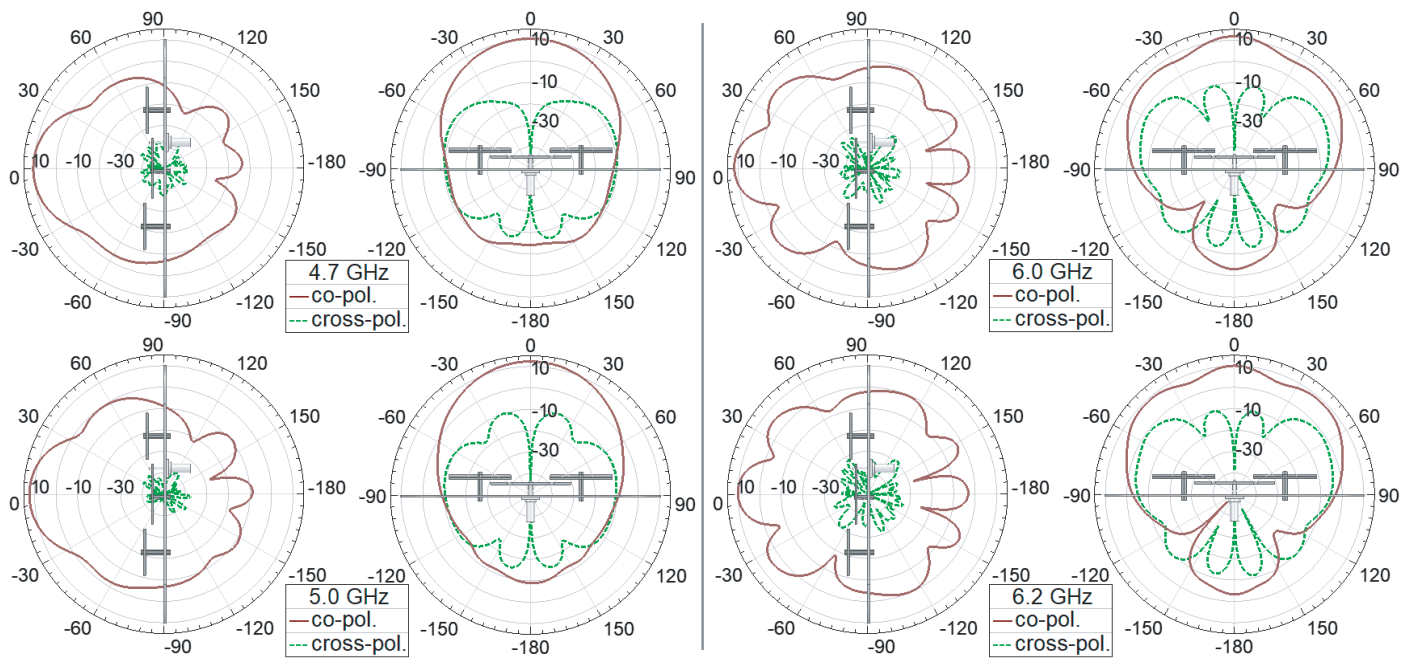

FIGURE 17. The simulated gain patterns of the optimized antenna with an E-shaped active exciter and four rectangular passive elements.

center of the active E-shaped exciter, as shown in Figure 14, which causes a change in the antenna's phase center. This effect can be useful where the use of a fixed electrical beam angle is appropriate, for example, when using the antenna as a base station antenna with preferential radio coverage in the lower hemisphere or as an antenna for a UAS GCS with preferential radio coverage in the upper hemisphere. However, some systems require an antenna without pattern deviation, that is, with a more stable phase center.

In order to mitigate the impact beam displacement, it is suggested that the metal stand in the model be substituted with a dielectric one. Figure 15 depict the distribution of currents and E-fields over the surfaces of the antenna exciters, derived from simulation results. We see a more uniform field distribution

TABLE 1. Comparison between the proposed design and the previous studies in high-gain patch antennas.

Source	Bandwidth (%) $S_{11} \leq -10\,\text{dB}$	Bandwidth (%) $S_{11} \leq -15\,\text{dB}$	Peak gain (dBi)	Average gain (dBi)	Overall size (λ_0)	Aperture efficiency (%)	Antenna Type
[5]	~ 33.0	~ 25.0	9.2	~ 8.5	$1.2 \times 1.2 \times 0.2$	~ 46	Modified ECPA on a suspended substrate
[31]	~ 15.9	–	12.5	~ 11.5	$1.5 \times 1.5 \times 0.03$	~ 63	4-element circularly polarized antenna array with parasitic patches
[32]	~ 87.0	–	9.5	~ 7.5	$0.8 \times 0.3 \times 0.3$	–	Crescent moon-shape patch-pair antenna
[33] Dual-Band	~ 81.6 ~ 30.4	–	8.1 12.5	~ 7.5 ~ 11.0	$0.4 \times 0.4 \times 0.3$ $1.1 \times 1.1 \times 0.7$	–	Bowtie antenna loaded with a square loop
[34]	~ 22.0	–	11.9	~ 10.5	$1.3 \times 1.3 \times 0.1$	~ 73	Pin-loaded patch antenna fed with a dual-mode SIW resonator
[35]	~ 44.6	~ 25.0	12.2	~ 10.0	$1.4 \times 1.5 \times 0.4$	~ 63	Microstrip antenna with folded ground walls
[36]	~ 19.4	~ 10.8	12.5	~ 11.2	$4.8 \times 1.3 \times 0.1$	~ 23	Double-walled SIW fractal slot and hexagonal ring slot linear antenna array
[37]	~ 57.1	~ 40.8	14.5	~ 12.5	$6.8 \times 0.75 \times 0.1$	~ 44	SIW leaky-wave antenna
[40]	~ 16.2	–	10.2	~ 9.4	$1.5 \times 1.5 \times 0.1$	~ 37	Antenna with 4 octagonal parasitic patches
[43]	~ 2.0	–	8.2	~ 8.0	$1.0 \times 1.0 \times 0.1$	~ 53	Patch antenna with one active and four parasitic circular elements
[45]	~ 6.9	–	8.2	~ 8.0	$1.0 \times 1.0 \times 0.1$	~ 53	LTCC microstrip parasitic patch antenna
[46]	~ 27.3	–	10.5	~ 9.0	$2.0 \times 1.6 \times 0.1$	~ 28	LTCC microstrip patch antenna array with parasitic surrounding stacked patches
Proposed	~ 7.0	~ 4.0	13.2	~ 12.5	$1.7 \times 1.7 \times 0.1$	~ 58	Rectangular active exciter and four rectangular passive elements
	~ 22.0	~ 14.0	13.1	~ 11.5	$1.7 \times 1.7 \times 0.1$	~ 58	U-shaped active exciter and four rectangular passive elements
	~ 33.0	~ 26.0	13.4	~ 12.2	$1.6 \times 1.6 \times 0.1$	~ 68	E-shaped active exciter and four rectangular passive elements

FIGURE 18. The simulated reflection coefficient magnitude of the optimized antenna with an E-shaped active exciter and four rectangular passive elements.

FIGURE 19. The simulated gain plot of the optimized antenna with an E-shaped active exciter and four rectangular passive elements.
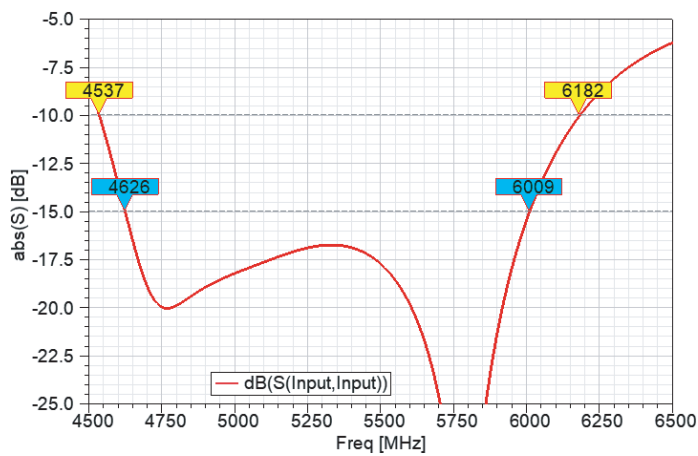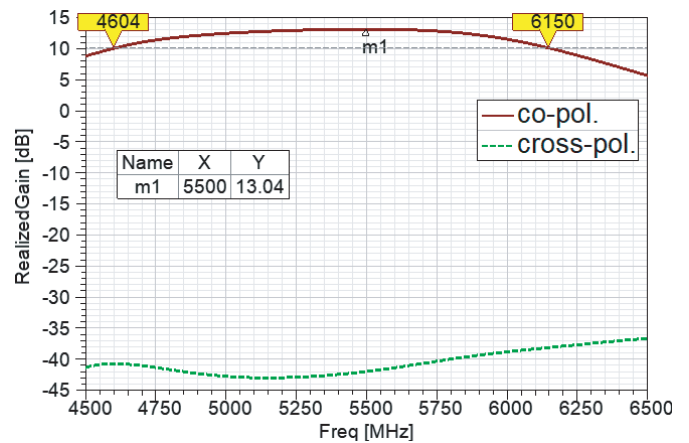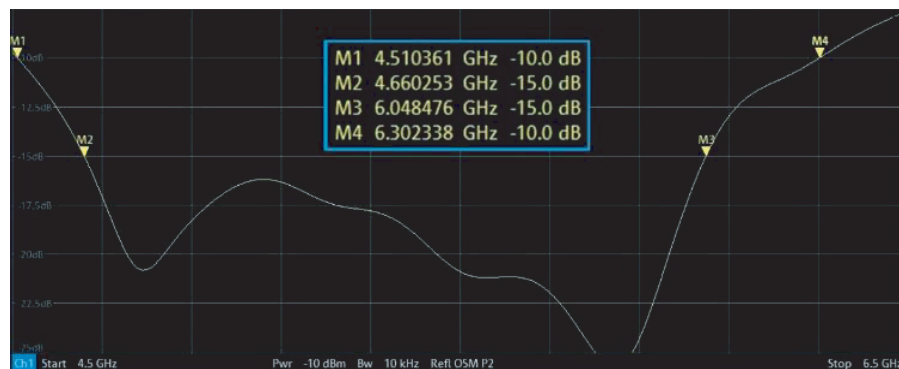

FIGURE 20. The measured reflection coefficient magnitude of the proposed wideband antenna with dielectric mounting rack under the active exciter.

across the antenna elements throughout the entire frequency range under consideration, from 4700 to 6200 MHz. In addition, the current vectors on the surfaces of the elements indicate a more stable phase center.

The antenna's input impedance varies along with changes in the characteristics of the rack used to place the active radiator. It is possible to adjust the antenna matching using slots in the active emitter by changing their lengths and the distance between them, Figure 16 shows the nature of these changes in the input characteristics of the antenna.

After adjusting the passive elements (dimensions, installation height, and distances between elements) in order to obtain the desired RP, it is possible to adjust the dimensions of the slots and match the antenna in the desired range at the required level.

5.4. Optimized High-Gain Antenna Based on the E-Shaped Active Exciter Simulation Results

The simulation results of the optimized high-gain antenna based on the E-shaped active exciter with four rectangular passive el-

ements and a dielectric mounting rack under the active exciter are shown in Figures 17–19.

The optimized high-gain antenna shows the following simulation results: the gain is 11–13 dBi in the wide frequency band 4707–6050 MHz (25%) with an impedance bandwidth matching of 15 dB; the working bandwidth is about 4537–6182 MHz (31%) with $|S_{11}| \leq -10$ dB and with the gain more than 9.5 dBi. The XPD exceeds 50 dB when being directed towards its maximum radiation in the whole frequency range of 4537–6182 MHz.

5.5. Optimized High-Gain Antenna Based on the E-Shaped Active Exciter Measurement Results

The measurement results of the optimized high-gain antenna based on the E-shaped active exciter with four rectangular passive elements and a dielectric mounting rack under the active exciter are shown in Figures 20 and 21.

Based on the data collected, the radiation patterns closely resemble those generated in the simulation; the measured impedance matching bandwidth is about 26% (4660–6048 MHz) with $|S_{11}| \leq -15$ dB and 33% (4510–6302 MHz)
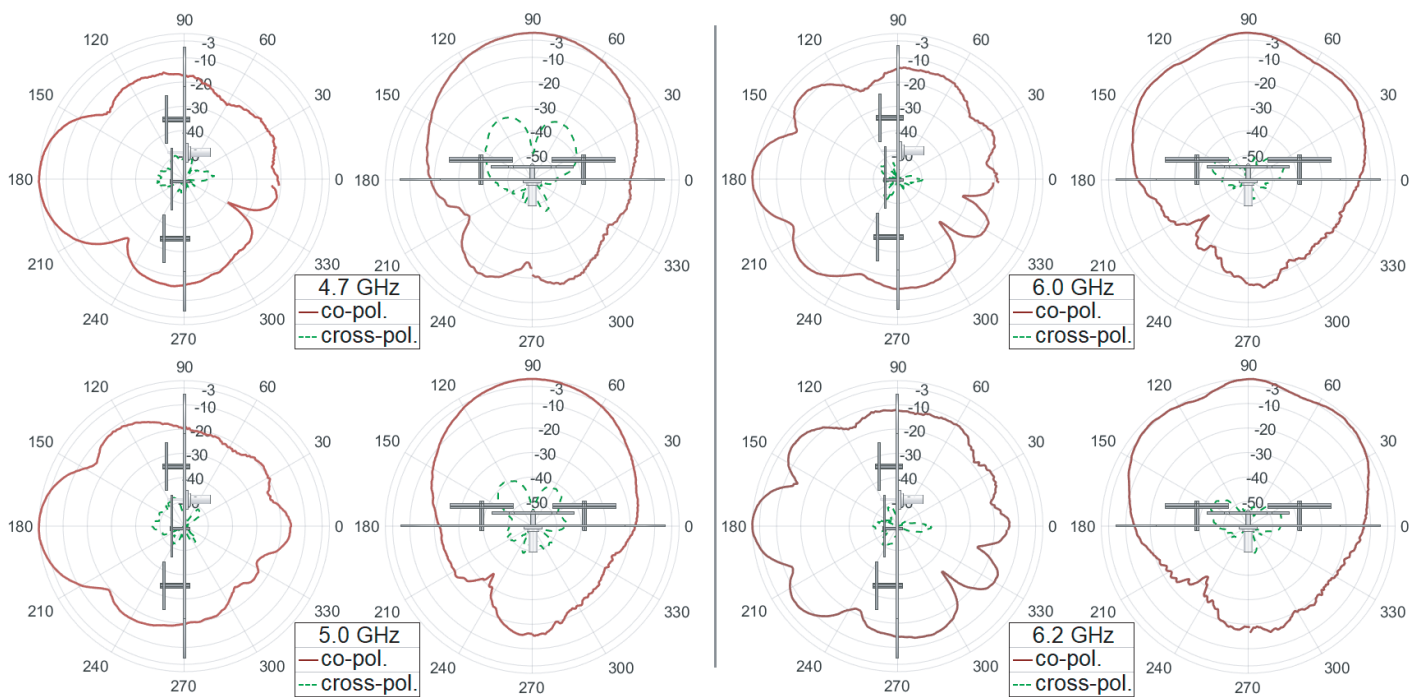
FIGURE 21. The radiation patterns of the proposed wideband antenna with dielectric mounting rack under the active exciter.
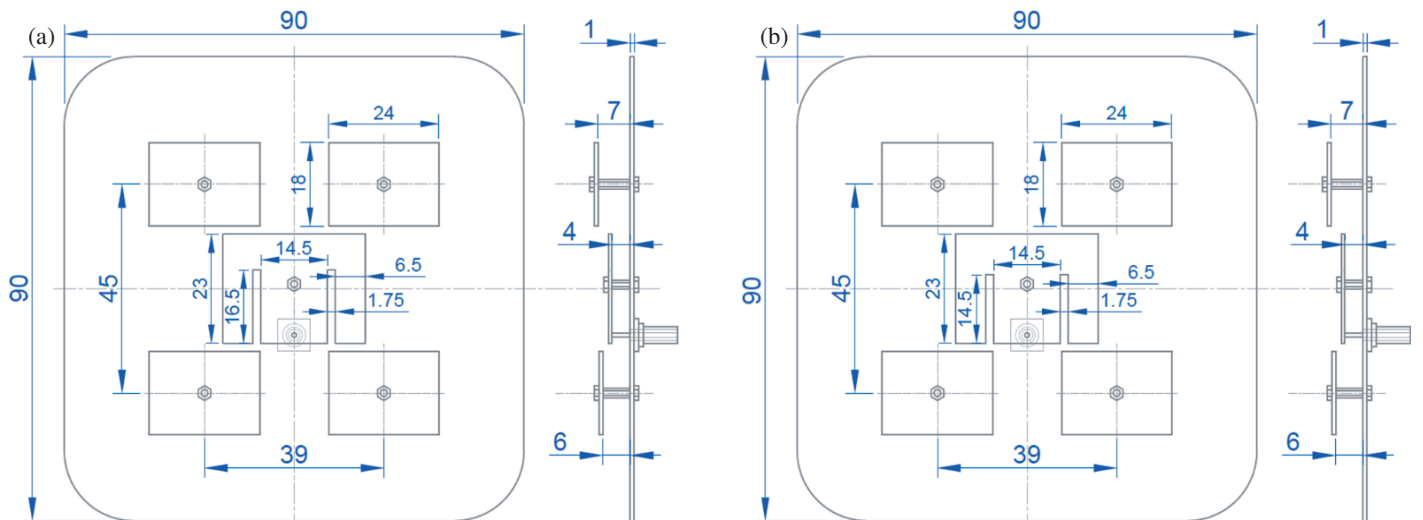

FIGURE 22. The proposed wideband antenna with (a) metal and (b) dielectric mounting rack under the active exciter.

with $|S_{11}| \leq -10$ dB; the measured maximum gain is 13.4 dBi at the 5500 MHz; the measured average gain is 12.2 dBi at the 4700–6200 MHz frequency band; the measured XPD exceeds 50 dB. The results of the measurements indicated strong antenna performance that aligned well with the simulation results.

Table 1 illustrates a comparison between the proposed antenna's characteristics and those of previously published developments. It is evident that the design, utilizing an E-shaped active exciter and four rectangular passive elements, demonstrates competitive features and the highest gain in small sizes.

6. CONCLUSION

The article presents an analysis of the possibilities of expanding the operating frequency band of an antenna based on an active rectangular exciter with the addition of four passive rectangular elements above the first one. Firstly, in contrast to the classical antenna from [44], it was proposed to place all the elements on racks without using a dielectric substrate, and secondly, based on the results of the analysis of the given design, it was suggested to expand the operating band of the antenna by replacing the active exciter with the following more wideband patches: the U-shaped and E-shaped patches.

Based on the analysis performed, a new wideband high-gain antenna design with linear polarization was proposed, whose performance was assessed based on modeling results in the ANSYS EM Suite (HFSS Design); subsequently, an antenna prototype was made, and its characteristics were measured. The presented antenna shows good performance in the wide frequency range: the measured impedance matching bandwidth is 26% (4660–6048 MHz) with $|S_{11}| \leq -15$ dB and 33% (4510–6302 MHz) with $|S_{11}| \leq -10$ dB; the measured maximum gain is 13.4 dBi at the 5500 MHz; the measured average gain is 12.2 dBi at the 4700–6200 MHz frequency band; and the measured XPD exceeds 50 dB. The antenna is small in size, about $1.6\lambda_0 \times 1.6\lambda_0 \times 0.1\lambda_0$, and its measured efficiency is about 68%. The design is quite simple to manufacture and stands out for its high strength, small size, and low cost. The proposed antenna may be designed with a different frequency band with a matching band of about 25% and can be used as a wireless communication system repeater or small cell antenna, as a GCS antenna in UAS, or for other wideband applications with high gain.

It is imperative to underscore the necessity for continued study of the proposed technique aimed at extending the operating frequency band of an antenna. For example, it is planned to consider the possibility of a greater expansion of the operating frequency band of the antenna while maintaining other characteristics, such as the possibility of obtaining dual-linear or circular polarization.

ACKNOWLEDGEMENT

APPENDIX A. PROPOSED ANTENNAS APPEARANCE WITH ITS DIMENSIONS

The appendix contains figure (Figure 22) showing the appearance of the antenna under study with dimensions in millimeters.

REFERENCES

[1] Shishkin, M. S., "Wideband high-gain dual-polarized antenna for 5G communications," in *2021 XV International Scientific-Technical Conference on Actual Problems Of Electronic Instrument Engineering (APEIE)*, 311–316, Novosibirsk, Russian Federation, Nov. 2021.

[2] Sullivan, P. and D. Schaubert, "Analysis of an aperture coupled microstrip antenna," *IEEE Transactions on Antennas and Propagation*, Vol. 34, No. 8, 977–984, 1986.

[3] Saed, M. A., "Efficient method for analysis and design of aperture-coupled rectangular microstrip antennas," *IEEE Transactions on Antennas and Propagation*, Vol. 41, No. 7, 986–988, 1993.

[4] Naji, D. K., J. S. Aziz, and R. S. Fyath, "Design and simulation of RFID aperture coupled fractal antennas," *International Journal of Engineering Business Management*, Vol. 4, 25, 2012.

[5] Shishkin, M. S. and S. N. Shabunin, "Analysis of various designs of wideband patch antennas," in *2022 IEEE International Multi-Conference on Engineering, Computer and Information*

Sciences (SIBIRCON), 1190–1193, Yekaterinburg, Russian Federation, Nov. 2022.

[6] Wong, K.-L., *Compact and Broadband Microstrip Antennas*, John Wiley & Sons, 2004.

[7] Kumar, A., A. Q. Ansari, B. K. Kanaujia, J. Kishor, and L. Matekovits, "A review on different techniques of mutual coupling reduction between elements of any MIMO antenna. Part 1: DGSs and parasitic structures," *Radio Science*, Vol. 56, No. 3, 1–25, 2021.

[8] Khidre, A., K. F. Lee, F. Yang, and A. Elsherbeni, "Wideband circularly polarized E-shaped patch antenna for wireless applications," *IEEE Antennas and Propagation Magazine*, Vol. 52, No. 5, 219–229, 2010.

[9] Awad, N. M. and M. K. Abdelazeez, "Multislot microstrip antenna for ultra-wide band applications," *Journal of King Saud University — Engineering Sciences*, Vol. 30, No. 1, 38–45, 2018.

[10] Kathuria, N. and S. Vashisht, "Dual-band printed slot antenna for the 5G wireless communication network," in *2016 International Conference on Wireless Communications, Signal Processing and Networking (WiSPNET)*, 1815–1817, Chennai, India, Mar. 2016.

[11] Najeeb, D., D. Hassan, R. Najeeb, and H. Ademgil, "Design and simulation of wideband microstrip patch antenna for RFID applications," in *2016 HONET-ICT*, 84–87, Nicosia, Cyprus, Oct. 2016.

[12] Vincenti Gatti, R., R. Rossi, and M. Dionigi, "Single-layer line-fed broadband microstrip patch antenna on thin substrates," *Electronics*, Vol. 10, No. 1, 37, 2021.

[13] Wi, S.-H., Y.-S. Lee, and J.-G. Yook, "Wideband microstrip patch antenna with U-shaped parasitic elements," *IEEE Transactions on Antennas and Propagation*, Vol. 55, No. 4, 1196–1199, 2007.

[14] Chen, Z. N., D. Liu, H. Nakano, X. Qing, and T. Zwick, *Handbook of Antenna Technologies*, Springer, 2016.

[15] Boufrioua, A., *Microstrip Antennas Modeling For Recent Applications*, Nova Science Publishers, 2016.

[16] Xu, K. D., H. Xu, Y. Liu, J. Li, and Q. H. Liu, "Microstrip patch antennas with multiple parasitic patches and shorting vias for bandwidth enhancement," *IEEE Access*, Vol. 6, 11 624–11 633, 2018.

[17] Tiwari, P., V. Gahlaut, M. Kaushik, A. Shastri, V. Arya, I. Elfergani, C. Zebiri, and J. Rodriguez, "Enhancing performance of millimeter wave MIMO antenna with a decoupling and common defected ground approach," *Technologies*, Vol. 11, No. 5, 142, 2023.

[18] Vadlamudi, R. and D. S. Kumar, "Nature stimulated dual band, dual polarized aerial with very good isolation for A-LTE/5G base station applications," in *2020 IEEE International Students' Conference on Electrical, Electronics and Computer Science (SCEECS)*, 1–3, Bhopal, India, Feb. 2020.

[19] Ta, S. X., D. M. Nguyen, K. K. Nguyen, C. D. Ngoc, and N. N. Trong, "Wideband differentially fed dual-polarized antenna for existing and sub-6 GHz 5G communications," *IEEE Antennas and Wireless Propagation Letters*, Vol. 19, No. 12, 2033–2037, 2020.

[20] Fernandez-Martinez, P., S. Martin-Anton, and D. Segovia-Vargas, "Design of a wideband Vivaldi antenna for 5G base stations," in *2019 IEEE International Symposium on Antennas and Propagation and USNC-URSI Radio Science Meeting*, 149–150, Atlanta, GA, USA, Jul. 2019.

[21] Jeong, Y.-Y. and W.-S. Lee, "Printed half bow-tie antenna array with four linear polarizations for UAV applications," in *2020 IEEE International Symposium on Antennas and Propagation and North American Radio Science Meeting*, 175–176, Montreal,

QC, Canada, Jul. 2020.

[22] Méndez, D. V. N., L. F. C. Suárez, and M. B. Escudero, "Antenna for satellite and UAV communications," in *2021 IEEE International Symposium on Antennas and Propagation and USNC-URSI Radio Science Meeting (APS/URSI)*, Singapore, Dec. 2021.

[23] Schulpen, R., U. Johannsen, S. C. Pires, and A. B. Smolders, "Design of a phased-array antenna for 5G base station applications in the 3.4-3.8 GHz band," in *12th European Conference on Antennas and Propagation (EuCAP 2018)*, London, UK, Apr. 2018.

[24] Hua, C., R. Li, Y. Wang, and Y. Lu, "Dual-polarized filtering antenna with printed jerusalem-cross radiator," *IEEE Access*, Vol. 6, 9000–9005, 2018.

[25] Kumar, A., M. Aljaidi, M. Singh, M. S. Alshammari, A. A. Alsuwaylimi, and S. M. Alenezi, "Recent trends in compact planar antennas at 5G sub-6 GHz and mmwave frequency bands for automotive wireless applications: A review," *Progress In Electromagnetics Research C*, Vol. 143, 169–180, 2024.

[26] Sokolov, V. S. and M. A. Stepanov, "MIMO 2 x 2 2.45 GHz antenna array with polarizing channel separation," in *2022 IEEE 23rd International Conference of Young Professionals in Electron Devices and Materials (EDM)*, 109–112, Altai, Russian Federation, Jun.-Jul. 2022.

[27] Wei, C.-H., T.-W. Chiou, and C.-J. Chuang, "Dual-band dual-polarization antenna array," in *2014 International Symposium on Antennas and Propagation Conference Proceedings*, 445–446, Kaohsiung, Taiwan, Dec. 2014.

[28] Ushijima, Y., E. Nishiyama, and M. Aikawa, "Dual-polarized microstrip array antenna with orthogonal feed circuit," in *2011 IEEE International Symposium on Antennas and Propagation (APSURSI)*, 561–564, Spokane, WA, USA, Jul. 2011.

[29] Ushijima, Y., E. Nishiyama, and M. Aikawa, "Single layer extensible microstrip array antenna integrating SPDT switch circuit for linear polarization switching," *IEEE Transactions on Antennas and Propagation*, Vol. 60, No. 11, 5447–5450, 2012.

[30] Alwareth, H., I. M. Ibrahim, Z. Zakaria, A. J. A. Al-Gburi, S. Ahmed, and Z. A. Nasser, "A wideband high-gain microstrip array antenna integrated with frequency-selective surface for sub-6 GHz 5G applications," *Micromachines*, Vol. 13, No. 8, 1215, 2022.

[31] Ding, K., C. Gao, T. Yu, D. Qu, and B. Zhang, "Gain-improved broadband circularly polarized antenna array with parasitic patches," *IEEE Antennas and Wireless Propagation Letters*, Vol. 16, 1468–1471, 2016.

[32] Guo, J., Y. Zou, and C. Liu, "Compact broadband crescent moon-shape patch-pair antenna," *IEEE Antennas and Wireless Propagation Letters*, Vol. 10, 435–437, 2011.

[33] Zhang, H., L. Chang, J. Zhang, and Z. Chen, "Dual band directional bowtie antenna loaded with a square loop," in *2016 11th International Symposium on Antennas, Propagation and EM Theory (ISAPE)*, 35–38, Guilin, China, Oct. 2016.

[34] Zhang, X., T.-Y. Tan, Q.-S. Wu, L. Zhu, S. Zhong, and T. Yuan, "Pin-loaded patch antenna fed with a dual-mode SIW resonator for bandwidth enhancement and stable high gain," *IEEE Antennas and Wireless Propagation Letters*, Vol. 20, No. 2, 279–283, 2021.

[35] Dhaundia, G. and K. J. Vinoy, "A high-gain wideband microstrip patch antenna with folded ground walls," *IEEE Antennas and Wireless Propagation Letters*, Vol. 22, No. 2, 377–381, 2023.

[36] Rabie, M. M., M. S. El-Gendy, A. R. Eldamak, F. Ibrahim, and H. El-Henawy, "Circularly polarized double-walled SIW fractal slot and hexagonal ring slot antenna array for X-band satellite applications," *Progress In Electromagnetics Research B*, Vol. 105, 1–15, 2024.

[37] Arya, V., T. Garg, and H. M. R. Al-Khafaji, "High gain and wide-angle continuous beam scanning SIW leaky-wave antenna," *Electronics*, Vol. 12, No. 2, 370, 2023.

[38] Kumar, G. and K. P. Ray, *Broadband Microstrip Antennas*, Artech House, 2002.

[39] Garg, R., *Microstrip Antenna Design Handbook*, Artech House, 2001.

[40] Kim, S.-W., H.-G. Yu, and D.-Y. Choi, "Analysis of patch antenna with broadband using octagon parasitic patch," *Sensors*, Vol. 21, No. 14, 4908, 2021.

[41] Akhter, Z., R. M. Bilal, and A. Shamim, "A dual mode, thin and wideband MIMO antenna system for seamless integration on UAV," *IEEE Open Journal of Antennas and Propagation*, Vol. 2, 991–1000, 2021.

[42] Cao, W.-Q. and W. Hong, "Bandwidth and gain enhancement for probe-fed CP microstrip antenna by loading with parasitical patches," *Progress In Electromagnetics Research Letters*, Vol. 61, 47–53, 2016.

[43] Jusoh, M., T. Sabapathy, M. F. Jamlos, and M. R. Kamarudin, "Reconfigurable four-parasitic-elements patch antenna for high-gain beam switching application," *IEEE Antennas and Wireless Propagation Letters*, Vol. 13, 79–82, 2014.

[44] Legay, H. and L. Shafai, "New stacked microstrip antenna with large bandwidth and high gain," *IEE Proceedings — Microwaves, Antennas and Propagation*, Vol. 141, No. 3, 199–204, 1994.

[45] Bunea, A.-C., D. Neculoiu, M. Lahti, and T. Vähä-Heikkilä, "LTCC microstrip parasitic patch antenna for 77 GHz automotive applications," in *2013 IEEE International Conference on Microwaves, Communications, Antennas and Electronic Systems (COMCAS 2013)*, 1–4, Tel Aviv, Israel, Oct. 2013.

[46] Lee, H.-J., E. S. Li, H. Jin, C.-Y. Li, and K.-S. Chin, "60 GHz wideband LTCC microstrip patch antenna array with parasitic surrounding stacked patches," *IET Microwaves, Antennas & Propagation*, Vol. 13, No. 1, 35–41, 2018.

[47] Zeng, Y., I. Guvenc, R. Zhang, G. Geraci, and D. W. Matolak, *UAV Communications for 5G and Beyond*, John Wiley & Sons, 2020.

[48] Shishkin, M. and S. Shabunin, "Design of a new antenna system for a meteorological radiosonde tracking radar," in *2021 Ural Symposium on Biomedical Engineering, Radioelectronics and Information Technology (USBEREIT)*, 0198–0201, Yekaterinburg, Russia, May 2021.

[49] Milligan, T. A., *Modern Antenna Design*, John Wiley & Sons, 2005.

[50] Balanis, C. A., *Antenna Theory: Analysis and Design*, John Wiley & Sons, 2016.